Genet Resour Crop Evol (2026) 73:202
https://doi.org/10.1007/s10722-026-02832-6

RESEARCH ARTICLE

Image-based phenotyping of faba bean genetic resources for water deficit responses under controlled conditions

Sylvain Poque · Ulrika Carlson-Nilsson · Muhammad Omer · Anna Palmé · Ingunn M. Vågen · Gert Poulsen · Matti W. Leino · Kristiina Himanen · Hamid Khazaei

Received: 3 May 2026 / Accepted: 23 May 2026

Abstract Faba bean (*Vicia faba* L.) has great potential to contribute to sustainable agriculture and protein security globally but is known to be very sensitive to drought stress. Uncovering drought-adapted germplasm is critical for developing resilient cultivars and advancing our understanding of the mechanisms underlying stress adaptation. However, high-throughput plant phenotyping under stress conditions remain a major bottleneck in crop genetics and breeding programs. In this study, a multi-sensor indoor phenotyping platform was used to assess 44 faba bean genotypes under water deficit conditions. Standardized, monitored stress conditions were achieved by watering-by-weighing for drought onset, duration, and intensities allowing genotype-level comparisons. The genotypes showed a range of stress responses in growth and physiology, including traits such as plant height, biomass, water use efficiency (WUE), and chlorophyll fluorescence parameters. Digital biomass, derived from combined top- and side-view plant imaging, was strongly correlated with biological biomass at the experimental endpoint, validating its use as a non-destructive proxy for growth assessment in faba bean. Time-resolved generalized additive modelling further revealed genotype-specific differences in the timing and magnitude of water deficit response. Genotypes that maintained growth and WUE under water deficit conditions may serve as valuable pre-breeding materials for development of drought-adapted faba bean.

Keywords Drought stress · Plant phenomics · Legumes · Digital biomass · Water use efficiency

Supplementary Information The online version contains supplementary material available at https://doi.org/10.1007/s10722-026-02832-6.

S. Poque · K. Himanen
National Plant Phenotyping Infrastructure, Organismal and Evolutionary Research Programme, Biocenter Finland, Helsinki Institute of Life Science, University of Helsinki, Helsinki, Finland

S. Poque · M. Omer · H. Khazaei (✉)
Department of Agricultural Sciences, University of Helsinki, Helsinki, Finland
e-mail: hamid.khazaei@luke.fi; hamid.khazaei@helsinki.fi

U. Carlson-Nilsson · A. Palmé
Nordic Genetic Resource Center (NordGen), Alnarp, Sweden

I. M. Vågen
Division Food Production and Society, Norwegian Institute of Bioeconomy Research (NIBIO), Ås, Norway

G. Poulsen
Frøsamlerne, Denmark

M. W. Leino
Archaeological Research Laboratory, Department of Archaeology and Classical Studies, Stockholm University, Stockholm, Sweden

H. Khazaei
Natural Resources Institute Finland, Helsinki, Finland

Published online: 02 June 2026

Introduction

Faba bean (*Vicia faba* L.) is an important cool-season grain legume crop grown worldwide because of its high seed protein content and versatility in agricultural systems, contributing to food security and sustainable agriculture (Jensen et al. 2010; Khazaei and Vandenberg 2020). Nevertheless, faba bean is considered to be sensitive to drought stress (Khan et al. 2010) as the major environmental factor that negatively affects its growth, development, and yield potential. Global climate change has dramatically changed the frequency and patterns of rainfall over the past few decades. The decrease in precipitation due to infrequent rain events, combined with the predicted rise in atmospheric temperature, intensifies the frequency and severity of drought incidents, negatively affecting crop performance (Spinoni et al. 2018; Bevacqua et al. 2022). For example, in the Nordic region, early- to mid-summer droughts have become extremely likely due to climate change and cause significant crop yield losses (Peltonen-Sainio et al. 2021). Therefore, development of drought-adapted cultivars is essential, particularly in drought-susceptible crops such as faba bean.

Plant phenotyping, the process of systematic measurement and analysis of plant traits, is fundamental to understanding plant-environment interactions (Pieruschka and Schurr 2019; Visakh et al. 2024). Through phenotyping in adequate conditions, drought-adapted germplasm can be identified to support the development of resilient cultivars and to advance understanding of stress adaptation mechanisms (Swarup et al. 2021). This requires systematic phenotyping of diverse genotypes under water-deficit conditions to identify those that exhibit superior production in water-limited environments (Guadarrama-Escobar et al. 2024). A number of faba bean genotypes have been screened for this purpose (e.g., Amede et al. 1999; Khazaei et al. 2013; Ali et al. 2016). However, these investigations have been largely constrained by the lack of reliable and standardized phenotyping tools and have often been conducted using low-throughput approaches.

High-Throughput Plant Phenotyping (HTPP) technologies have revolutionized plant breeding by enabling rapid, precise, and large-scale assessment of plant traits under controlled and field conditions. The HTPP platforms leverage advanced imaging technologies, such as visible light RedGreenBlue (RGB) imaging, thermal imaging, hyperspectral imaging, and chlorophyll fluorometry, to provide detailed insights into the physiological, morphological, and biochemical responses of plants to drought stress (Kim et al. 2021; Gill et al. 2022; Mansoor and Chung 2024; Sozzani et al. 2014). The HTPP facilitates the characterization of key traits related to shoot and root architecture (Nagel et al. 2012), and physiological adaptation to water stress (Shapiguzov et al. 2026). These platforms allow researchers to identify drought adapted germplasm and enhance genetic research by integrating phenotyping and genotyping data (Roitch et al. 2022; Al-Tamimi et al. 2022; Anshori et al. 2023). Integrated image analysis and machine learning has recently enabled the assessment of large populations of faba bean under natural field conditions (Ji et al. 2024). Furthermore, digital phenotyping tools and protocols, for example to measure digital biomass, have been more developed and applied in cereals (Neumann et al. 2015; Dodig et al. 2021) than in grain legumes.

Despite the potential of HTPP technologies, field-based phenotyping remains resource-intensive and is often challenged by the inherent variability in drought onset, duration, and intensity. To address these challenges, researchers have employed innovative approaches such as mobile field rainout shelters (Mohammadi et al. 2024; Balko et al. 2023). Outdoor and indoor HTPP approaches are complementary, as indoor facilities enable controlled, high-precision monitoring of plant traits under controlled environmental conditions, while outdoor platforms capture plant performance under field conditions.

To better understand the response of faba bean above-ground to water deficit, we utilized an indoor HTPP facility, which allowed automated watering and precise water deficit treatment. The National Plant Phenotyping Infrastructure (NaPPI), a state-of-the-art indoor facility at the University of Helsinki, Finland, was used to monitor plant stress responses using visible-light RGB cameras and chlorophyll fluorometry (Alexandersson et al. 2018; Pollari et al. 2022; Chovancek et al. 2025). The aims of this study were to (i) characterise phenotypic variation in a faba bean germplasm collection for growth dynamics, biological and digital biomass, water use efficiency (WUE), and chlorophyll fluorescence parameters under well watered and water deficit; (ii) assess the potential of

image-derived digital biomass and digital WUE to function as non-destructive proxies for their biological counterparts in this species, and (iii) apply time-resolved generalized additive modelling to classify genotypes by the timing of growth responses to water deficit.

Materials and methods

Plant material

Forty-four faba bean genotypes were used in this study. Information on genotype identification, origin and collection sites are presented in Table S1. The material includes both large-seeded garden types and smaller seeded fodder types and originated from Nordic countries and northern Europe. Seed of landraces from Finland and Sweden (Leino 2023) were directly obtained from the Nordic genebank (NordGen; Alnarp, Sweden). Genotypes ILB 938/2 and Mélodie/2 were added to the set as benchmarks for high water use efficiency and Aurora/2 as a cultivar with low water use efficiency (Khazaei et al. 2014 and 2018).

Growing conditions

The plants were grown in a plexiglass greenhouse within the Viikki Plant Growth Facilities (ViGOR), University of Helsinki, Finland. The growth conditions were set to a 16h light and 8h dark photoperiod, with day and night air temperatures set at 21 C and 16 C, respectively, and a target relative humidity (RH) of approximately 60%. A photosynthetic photon flux density of approximately 250–300 µmol. $m^{-2}.s^{-1}$ was maintained at the canopy level by high-pressure sodium lamps. Environmental conditions inside the greenhouse were logged every minute throughout the experiment. Across the experimental period, mean daytime values were 22.8 °C, 46.1% RH; mean nighttime values were 18.9 °C and 55.4% RH. The corresponding mean vapour pressure deficit (VPD) was 1.53 kPa during the day and 0.99 kPa at night, indicating moderate to occasionally high evaporative demand. All conditions were uniform across treatments and genotypes. Seeds of all 44 genotypes were sown in three batches in October 2024, in 5 L pots filled with peat-based potting mix (Karkea Ruukutusseos, W R8014, Kekkilä Oy, Vantaa, Finland). Before sowing, they were inoculated with *Rhizobium leguminosarum* biovar. *viciae* (Elomestari Oy, Tornio, Finland). The 264 pots were divided into three batches each containing one pot (having 1 plant) for the well watered treatment and one for the water deficit treatment. To minimise potential positional effects within the greenhouse, pots were assigned to positions within each batch in a fully randomised order at the start of the experiment. Batches were then rotated weekly across greenhouse positions as a unit, ensuring that no batch remained in the same spatial position for more than one week throughout the experiment.

Water deficit treatment

During the first seven days after germination (DAG), all the pots were watered to reach field capacity to allow proper seed germination. Prior to the experiment, the water holding capacity (WHC) of the peat was determined by weighing equally soil filled pots, saturated with water and allowed to drain freely for 24h (equivalent to field capacity), representing 100% of the WHC. Then the same pots were completely oven-dried to 0% of the WHC and weighed. These established the relationship between pot weight and actual water content (%) used to monitor soil WHC% during the experiment (Figure S1). For the experiment the soil in each pot was weighed to ensure uniformity. This standardized approach minimized variation in soil volume, providing consistent water levels for all plants. The pots were covered with blue mat to limit evaporation and facilitate plant imaging. Automated watering by weighing allowed daily recording of pot weights, enabling calculation of both water loss between consecutive days (g) and the amount of water supplied. The plants were subsequently subjected to two distinct water regimes: 80% of the WHC as the control treatment and 30% of the WHC as the water deficit treatment, which was gradually achieved by 20 DAG. The 30% WHC level was selected based on preliminary trials in which 25% WHC caused excessive stress and rapid decline in several genotypes, whereas 30% WHC produced a stable, moderate drought level suitable for differentiating genotype responses without inducing premature plant failure. These watering levels were maintained for 10 days (Fig. 1). After 31 DAG, the water deficit treatment was intensified

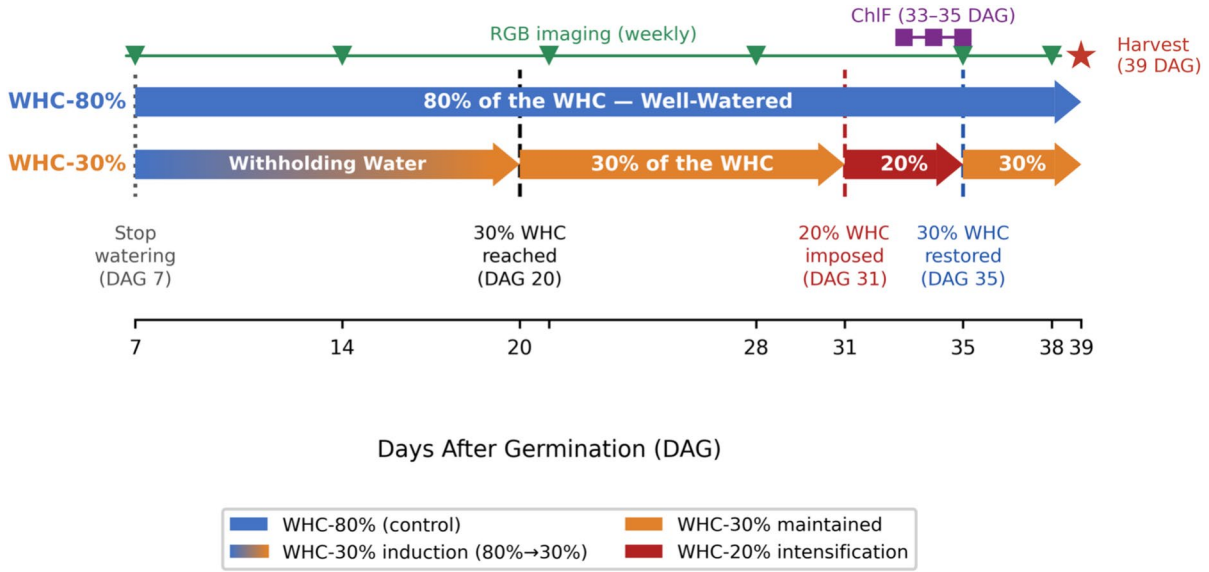

Fig. 1 Water stress treatment and measurements during the experiment. Two treatments were maintained from days after germination (DAG) 7 until harvest at DAG 39: a well-watered control (WHC-80%, upper track, blue) held continuously at 80% of the water-holding capacity (WHC), and water deficit treatment (lower track) underwent progressive water withholding from DAG 7, reaching 30% of the WHC at DAG 20 (gradient shading indicates the induction period), which was then maintained until DAG 31. A transient intensification to 20% of the WHC was imposed between DAG 31 and DAG 35 (dark red), after which soil water content was restored to 30% of the WHC until harvest. RGB canopy imaging was performed weekly (green triangles), chlorophyll fluorescence (ChlF) measurements on three consecutive days (DAG 33–35; purple squares), and plants harvested at DAG 39 (red star). Dashed vertical lines indicate key treatment transitions

by reducing the water level to 20% of the WHC for 5 days, in order to amplify stress severity and capture a broader range of genotypic responses. This step was planned before the experiment nontheless the timing and duration were adjusted in real time based on daily plant monitoring. By 35 DAG, WHC was adjusted back to 30% and maintained at this level until 39 DAG (Fig. 1 and Figure S1).

Image-based phenotyping

The phenotyping was performed at the National Plant Phenotyping Infrastructure (NaPPI, http://www.helsinki.fi/en/infrastructures/national-plant-phenotyping). The PlantScreen™ Modular platform is an integrated system for automated plant imaging and management. Plants are set in individual transportation disks and moved between handling, imaging and watering stations. The feature of watering by weighing allows for management of water content of the soil (Chovancek et al. 2025). This phenotyping platform is equipped with imaging units, for top- and side-view visible light RGBs and top-view pulse amplitude modulated (PAM) chlorophyll fluorometer (FluorCam). Lighting conditions, plant positioning, and camera settings were fixed throughout the experiment. All imaging and chlorophyll fluorescence sessions were initiated at 07:00, one hour after the onset of the light period, ensuring consistent time-of-day conditions across measurements.

Visible-light digital imaging

The RGB imaging unit is a light-isolated box equipped with a turning table with precise angle positioning, RGB cameras using GigE uEye UI-5480SE-C/M-5 Megapixels QSXGA Camera with 1/2″ CMOS Sensor (IDS, Germany) are supplemented with LED-based lighting source to ensure homogenous illumination of the imaged object. Top view RGB images of the plants were captured at resolution 2560 × 1920 pixels and camera height was automatically adjusted by a light curtain unit measuring plant height. For side view projections, line scan camera captured

images at resolution of 2560 × 3476 pixels. Weekly RGB imaging was performed for all plants, with additional imaging of individual batches conducted separately within the same week, for more than five weeks. Top and side view RGB imaging were used to capture plant growth parameters such as the canopy area, side view area and height during the time series. The plant surface area was segmented using pixel colour thresholding of the RGB images and all growth parameters were automatically analysed by PlantScreen Data Analyzer v3.2.4.5 (PSI, Drásov, Czech R.). To facilitate top-view canopy data extraction, blue rubber mats were placed around each plant in each pot. Representative examples of segmented side-view and top-view images under both watering treatments are shown in Figure S2. During the experiment plant height was determined using the extraction from the side-view images (RGB1) by counting the distance between the lowest and highest pixels. For RGB1, three photos were taken at each time point, with two 120º rotations of the plant between each imaging. Any morphological parameters associated with side views were calculated as the average of values derived from the three-angles (0º, 120º, and 240º).

Chlorophyll fluorescence measurements

A top-view Pulse Amplitude Modulated (PAM) chlorophyll a fluorometer (FluorCam FC-800MF, PSI, Czech Republic), equipped with a dark-adaptation tunnel and an imaging area of 800 × 800 mm, was used for chlorophyll fluorescence (ChlF) measurements (Tschiersch et al. 2017). The ChlF imaging was used to monitor plant physiological responses under well watered and water-deficit conditions by assessing parameters indicative of photosynthetic efficiency, including the quantum yield of PSII (QY) and stress-induced heat dissipation, measured as non-photochemical quenching (NPQ). Measurements were distributed across three batches over three consecutive days over a period of five weeks.

The ChlF parameters were determined after a 30-min dark period using a quenching protocol developed with FluorCam 7.0 software (PSI, Drásov, Czech R.). The quenching protocol consisted of two phases: initial dark phase and actinic light phase. In the initial dark-adapted phase, after measuring the minimal fluorescence (Fo), a saturating pulse was applied to determine the maximum fluorescence (Fm). The variable fluorescence (Fv, calculated as Fm – Fo) was then divided by Fm to obtain the maximum PSII quantum yield (Fv/Fm). During the subsequent light-adapted phase, actinic light was applied, and saturating pulses were used to determine the maximum fluorescence under light (Fm′) and the steady-state fluorescence (Fs). The effective quantum yield of PSII at light steady state (QY_Lss) was calculated as $(Fm' - Fs)/Fm'$, providing an estimate of the fraction of absorbed light energy used for photochemistry. Non-photochemical quenching at light steady state (NPQ_Lss) was calculated as $(Fm - Fm')/Fm'$, providing a measure of the regulated dissipation of excess excitation energy as heat (Horton and Ruban 1992).

Calculated parameters

Image-based measurements were used to derive several traits that quantify plant responses to drought stress. To enable meaningful comparisons across genotypes, normalized plant height and digital biomass were calculated. These represent the relative change, expressed as a percentage, between water deficit (WHC-30%) and well watered (WHC-80%) conditions, capturing the extent of growth reduction due to limited water availability.

The normalized plant height was calculated as:

$$\textit{Normalized plant height}\,(\%) = ((\textit{plant height of WHC} - 30\%/\textit{plant height of WHC} - 80\%) - 1) \times 100$$

Digital biomass was calculated by combining pixel areas extracted from three side-view and one top-view image as an arbitrary volumetric measurement (Rahaman et al. 2017). Digital biomass is calculated as:

$$\textit{Digital biomass} = \sqrt{(\textit{average of three side view areas})^2 \times \textit{top area}}$$

Normalized digital biomass, recorded on the final day of the experiment, were calculated as:

$$\textit{Normalized digital biomass}\,(\%) = ((\textit{digital biomass of WHC} - 30\% \,/\, \textit{digital biomass of WHC} - 80\%) - 1) \times 100$$

*Biological biomass (fresh weight and dry matter)*For the endpoint measurements at 39 DAG, the above-ground parts of the plants were collected into paper bags, and their fresh weights were recorded with a Mettler PM480 balance (GWB, Germany). After this, the plants were dried in a sample oven at 80 °C for 72h, and the dry matter content was recorded on the same balance after two weeks. These two endpoint measurements represent so-called biological biomass in our study: biological biomass (FW) for fresh weight and biological biomass (DM) for dry matter.

Water use efficiency (WUE)

Daily watering by weighing allowed recording of the total amount of water given to each plant from 4 to 39 DAGs. We determined the biological WUE by dividing the endpoint biological biomass (DM) produced (g) by the total amount of water (kg) supplied until 39 DAG. To establish non-destructive method for the same a digital WUE was calculated by dividing the digital biomass (volume) by the total amount of water (kg) provided until 37 DAG, *i.e.,* one day prior to imaging at 38 DAG.

Data analysis

Each RGB image underwent a fisheye correction and background exclusion. Data Analyzer v.3.4.17.3 (PSI, Drásov, Czech Republic) was used to manage the original images and data and their storage in the database. Canopy area, side-view areas, and height data were extracted from the green pixel measurements by MorphoAnalysis v.1.0.14.4 software (PSI, Drásov, Czech Republic). The ChlF data were analyzed via FluorCam 7 software (PSI.cz). The numerical data were processed via homemade pipelines via Python 3.13 (https://www.python.org). Two-way ANOVA was performed in JMP Pro 18, with genotype and treatment as fixed factors ($n = 3$ replicates per genotype × treatment combination, corresponding to the three sowing batches). All bar plots were generated using the Seaborn library (Waskom 2021). Pairwise differences among genotypes were assessed using Tukey's honest significant difference (HSD) post-hoc test, with compact letter displays (CLDs) generated via the split-then-absorb algorithm (Piepho 2004) implemented through the pairwise_tukeyhsd function in the Python statsmodels package ($\alpha = 0.05$). In figures, bars sharing the same letter are not significantly different from one another, while between-treatment differences for each accession were assessed using Welch's t-test; significance is indicated by brackets above each genotype pair.

GAM modelling

To assess the dynamic response of genotypes under water deficit, we applied generalized additive models (GAMs) with an autoregressive error structure. For each genotype and treatment conditions, a GAM was fitted using the *mgcv* package in R (Wood 2011), based on plant height and digital biomass data. The model residuals were inspected for temporal autocorrelation using the estimated lag-1 autocorrelation coefficient (ρ). When ρ exceeded 0.2, the model was refitted using mgcv::bam() including a first-order autoregressive [AR(1)] term to account for serial dependence across measurement days. This correction was applied to models for both plant height and digital biomass across all 44 genotypes, as all genotypes exceeded the $\rho > 0.2$ threshold in both traits (plant height: $\rho = 0.458$–0.775; digital biomass: $\rho = 0.360$–0.828). To quantify treatment effects, we used the plot_diff function from the *itsadug* package (van Rij et al. 2022) to estimate pointwise differences between WHC-30% and WHC-80% smooths across DAG, evaluated at 100 equally spaced time points. The difference was considered significant when its 95% confidence interval did not overlap zero. For plant height, the onset of divergence, defined as the first evaluated time point at which the lower bound of the 95% CI exceeded zero, was recorded as the drought impact day for each genotype, and genotypes were classified as early responders (divergence ≤ 20 DAG) or late responders (divergence > 20 DAG). This threshold corresponds to the day at which the WHC-30% treatment level was first achieved (Fig. 1), and coincides with a natural break in the observed distribution of onset days. The precision of this onset estimate is bounded by the evaluation grid resolution (~0.35 DAG per step), representing the maximum timing uncertainty for any genotype. Smooth response curves were visualized alongside observed

means and standard deviations using ggplot2 (Wickham 2016). All analyses were conducted in R version 4.3.3 (R Core Team 2025).

Results

Plant height

Water deficit treatment significantly reduced plant height for all the studied genotypes ($P < 0.001$; Table S2a), as visualized by the GAM-modelled trajectories in Figure S3. The pointwise difference for plant height among genotypes in well watered and water deficit treatments, estimated from the fitted GAM smooths, are presented in Figure S4, expressed in absolute units (cm), as the purpose of this analysis is to identify the day of significant treatment divergence rather than to compare genotypes by the magnitude of their drought response. Based on the first day of significant divergence, half of the genotypes showed an onset of treatment divergence before 20 DAG. In contrast, some genotypes such as Romfartuna, Lövånger, and Dalabona responded after 20 DAG to water deficit (Fig. 2). The results showed that water deficit treatment caused significant reduction in normalized plant height. Among the studied genotypes,

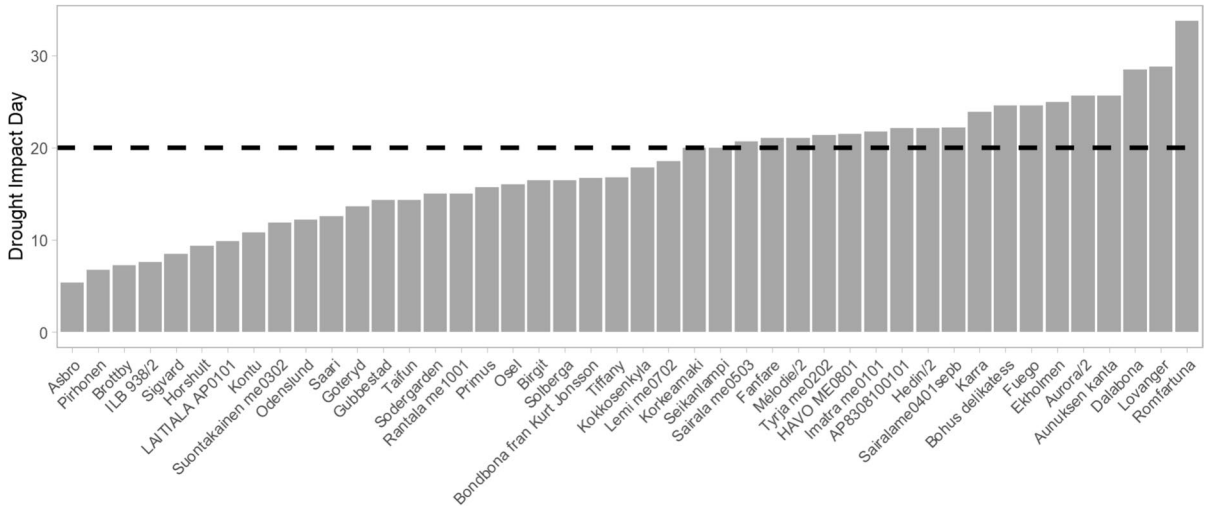

Fig. 2 Bar plot showing days after germination (DAG) of the water deficit impact on plant height. Significance of divergence in plant height between the two water holding capacity treatments was determined using pairwise comparisons of fitted smooths from generalized additive models. The dashed black line indicates 20 DAG, corresponding to the time when the water-deficit level was reached

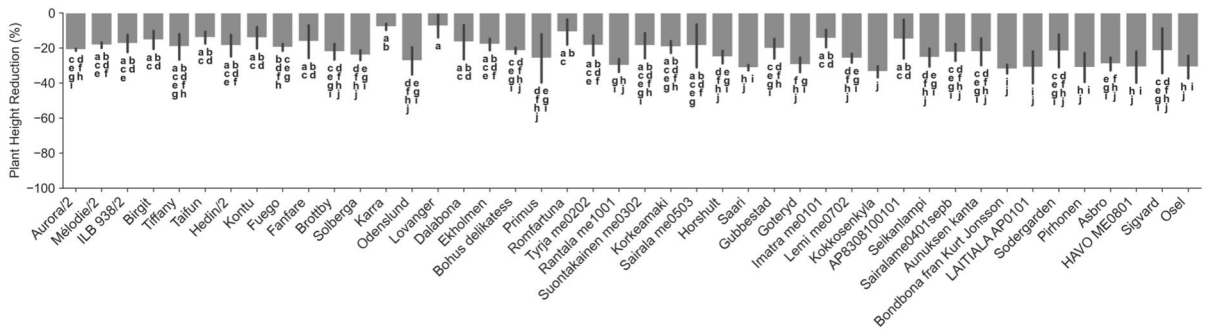

Fig. 3 Average normalized plant height (±SD) at the end point (38 DAG) among 44 faba bean genotypes under water deficit (WHC-30%). Bars sharing the same letter are not significantly different (Tukey's HSD, $\alpha = 0.05$)

Lövånger, Kärra, Romfartuna, Imatra me0101, and AP8308100101 had lowest reduction in normalized plant height under water deficit conditions (Table S2b; Fig. 3).

Digital biomass

Water deficit treatment significantly reduced digital biomass for all the studied genotypes ($P < 0.001$) (Table S2a). For all genotypes the digital biomass was calculated as time series under both well watered and water deficit conditions (Figure S5). Among the studied genotypes, Romfartuna, and Primus had lowest reduction in digital biomass under water deficit conditions (Fig. 4).

Biological WUE

Under water deficit conditions, ILB 938/2 and Mélodie/2 (our reference genotypes for high WUE) had significantly higher biological WUE in both well watered and water deficit treatments than

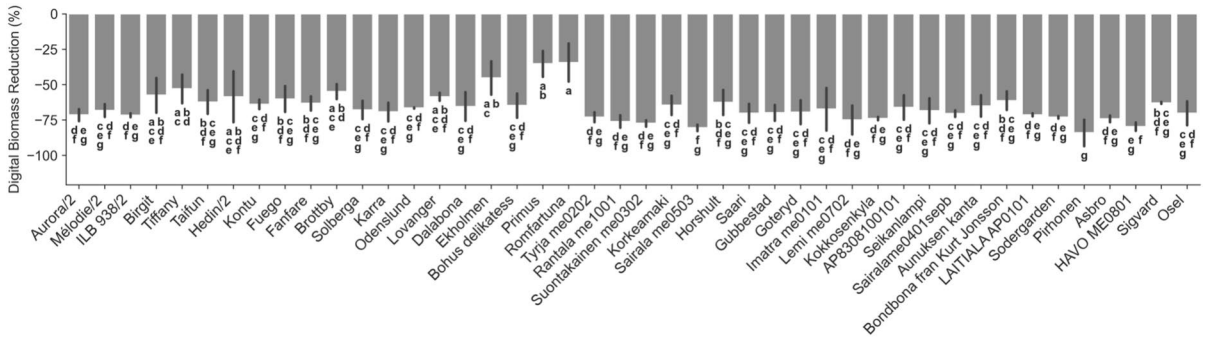

Fig. 4 Average normalized digital biomass (±SD) at the end point (38 DAG) among the 44 faba bean genotypes under water deficit (WHC-30%). Bars sharing the same letter are not significantly different (Tukey's HSD, $\alpha = 0.05$)

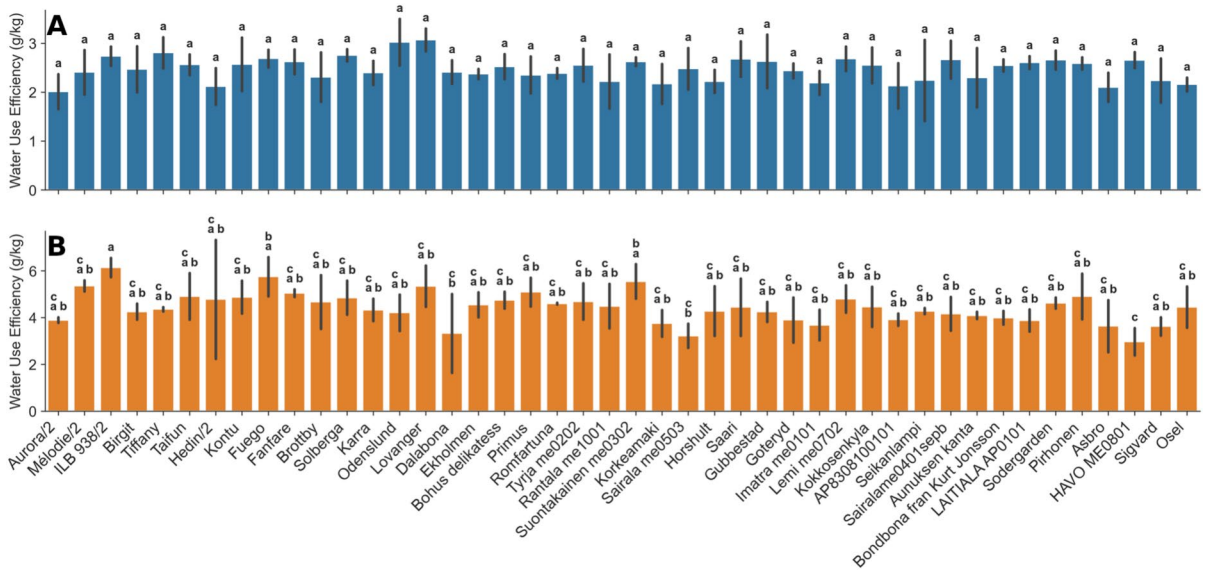

Fig. 5 Average biological water use efficiency (±SD) among 44 faba bean genotypes **A** under well watered (WHC-80%) and **B** water deficit (WHC-30%) conditions. Within each treatment, bars sharing the same letter are not significantly different (Tukey's HSD, $\alpha = 0.05$)

Aurora (reference genotype for low WUE) (Fig. 5; Table S2b). Genotypes Lövånger, Fuego, and Suontakainen me0302 had highest biological WUE under water deficit conditions, although pairwise comparisons did not reveal statistically significant differences from all other genotypes (Table S2b; Fig. 5).

Digital WUE

Similar to biological WUE, the digital WUE significantly varied across all faba bean genotypes (Table S2b). Under water-deficit conditions, ILB 938/2 ranked among the genotypes with high digital WUE, while Aurora/2 is among those with the lowest value (Fig. 6). However, not all genotypes followed the same trend as observed for the biological WUE.

Chlorophyll fluorescence imaging

The ChlF measurements among all faba bean genotypes showed significant reduction in the effective quantum yield (QY_Lss) and an increase in non-photochemical quenching (NPQ_Lss) parameters, indicative of photosynthetic efficiency and stress induced heat dissipation, respectively (Fig. 7; Table S2a and b).

Relationships among the studied parameters

The correlation matrix is presented in Fig. 8 showing the relationships among studied parameters. Both digital biomass and biological biomass were measured and correlated among the endpoint measurements, including biological biomass (FW), biological biomass (DM), and other measured traits between the two water treatments. Digital biomass showed strong correlations with both biological biomass (DM) ($r=0.71$) and biological biomass (FW) ($r=0.66$) under water deficit conditions, and even stronger correlations under well watered conditions ($r=0.74$). In contrast, plant height showed only a moderate correlation with biomass traits [biological biomass (FW): $r=0.31$–0.42 (water deficit and well watered conditions, respectively); biological biomass (DM): $r=0.47$–0.53 (water deficit and well watered conditions, respectively)], indicating its limited reliability as a predictor of final biomass. Digital WUE showed only moderate correlation with biological WUE under water deficit conditions ($r=0.56$). The ChlF

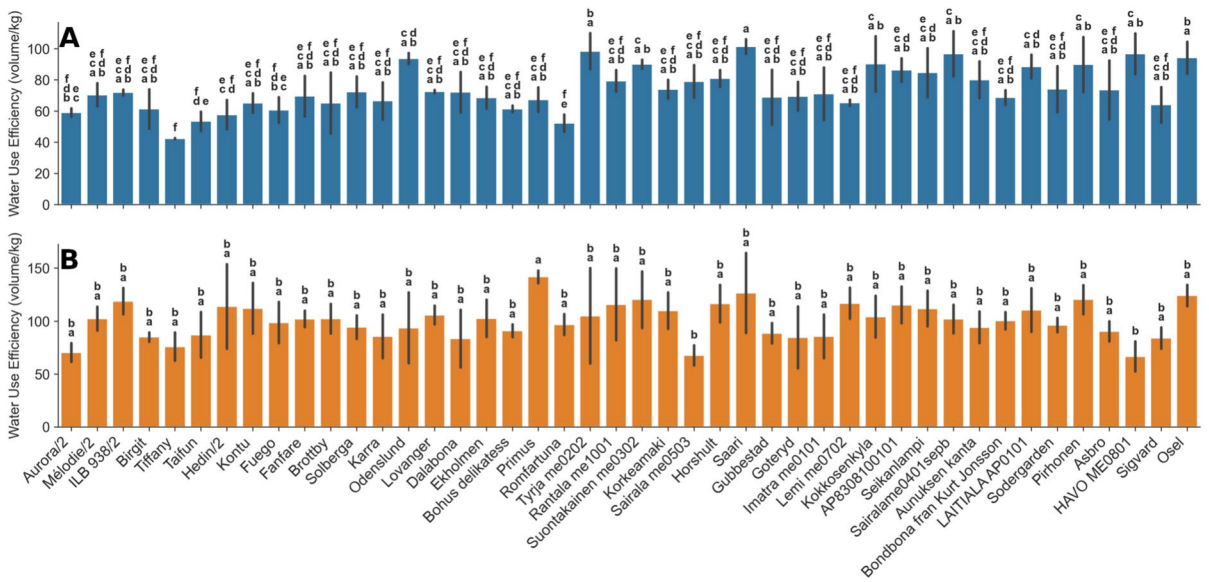

Fig. 6 Average digital water use efficiency (±SD) calculated as digital biomass (volume) divided by total water consumed (kg) until 38 DAG, among 44 faba bean genotypes **A** under well watered (WHC-80%) and **B** water deficit (WHC-30%) conditions. Within each treatment, bars sharing the same letter are not significantly different (Tukey's HSD, $\alpha=0.05$)

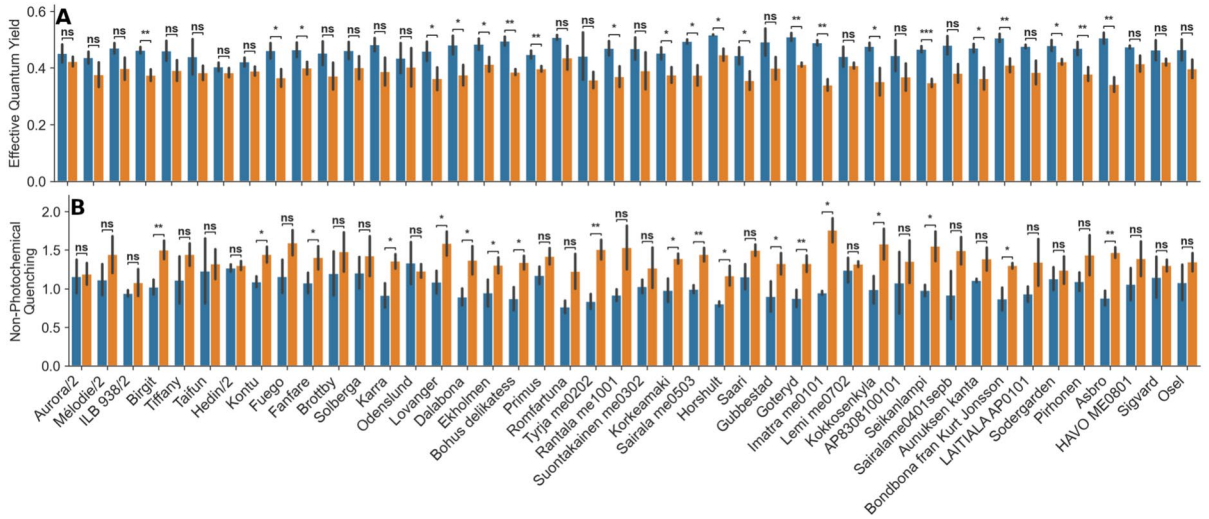

Fig. 7 Chlorophyll fluorescence measured at 39 days after germination under well watered (blue) and water deficit (orange) conditions. **A** Effective quantum yield of PSII at light steady state (QY_Lss). **B** Non-photochemical quenching at light steady state (NPQ_Lss). Brackets above each accession indicate significant between-treatment differences (Welch's t-test: $*P < 0.05$, $**P < 0.01$, $***P < 0.001$; ns, not significant)

parameters showed overall weak correlations with the morphological traits under water deficit conditions.

Discussion

Here, we present a case study in which a relatively large faba bean germplasm collection was subjected to water deficit stress screened in a controlled environment, by using advanced imaging technologies. Building on multi-side imaging capabilities, we explored for the first time how digital biomass correlates with traditional biological measurements in faba bean. Our results revealed a strong positive correlation between the digital and biological biomass at the endpoint, validating that digital biomass can serve as a proxy for assessing the plant growth responses of faba bean during water deficit in controlled environments. Importantly, this relationship reflects phenotypic variation under imposed stress rather than intrinsic superiority of genotypes under field drought conditions. Digital biomass derived from digital top- and side-view images has been used to predict plant biological biomass evolution in barley and maize (e.g., Klukas et al. 2014; Chen et al. 2014; Neumann et al. 2015) and to monitor the effects of biostimulants on drought stress in tomatoes (e.g., Chovancek et al. 2025) and the salinity response in safflower (Thoday-Kennedy et al. 2021).

WUE is one of the key traits in drought adaptation, as it reflects a plant's ability to maintain productivity under limited water availability (Blum 2009). High WUE indicates that a plant can assimilate more biomass per unit of water consumed, making it a valuable target for breeding crops better adapted to water-limited environments. WUE is a complex trait, and it is highly influenced by multiple physiological and morphological factors. An increase in WUE does not always translate directly into higher yield under field conditions (e.g., Hatfield and Dold 2019). In this study, we used ILB 938/2 and Mélodie/2 as known genotypes with high WUE and Aurora/2 as a poor WUE genotype (Khazaei et al. 2013; Khan et al. 2007; Mandour et al. 2023). Our results confirmed that these genotypes maintained their expected WUE also under controlled growing conditions. This highlights the ability of the phenotyping facility to screen a germplasm collection. The digital biomass and precise recording of the watering events during the entire experiment allowed us to calculate digital WUE but it was only moderately correlated with biological WUE under water deficit condition, indicating important limitations in its use as a proxy. This discrepancy likely reflects differences in tissue density that are not

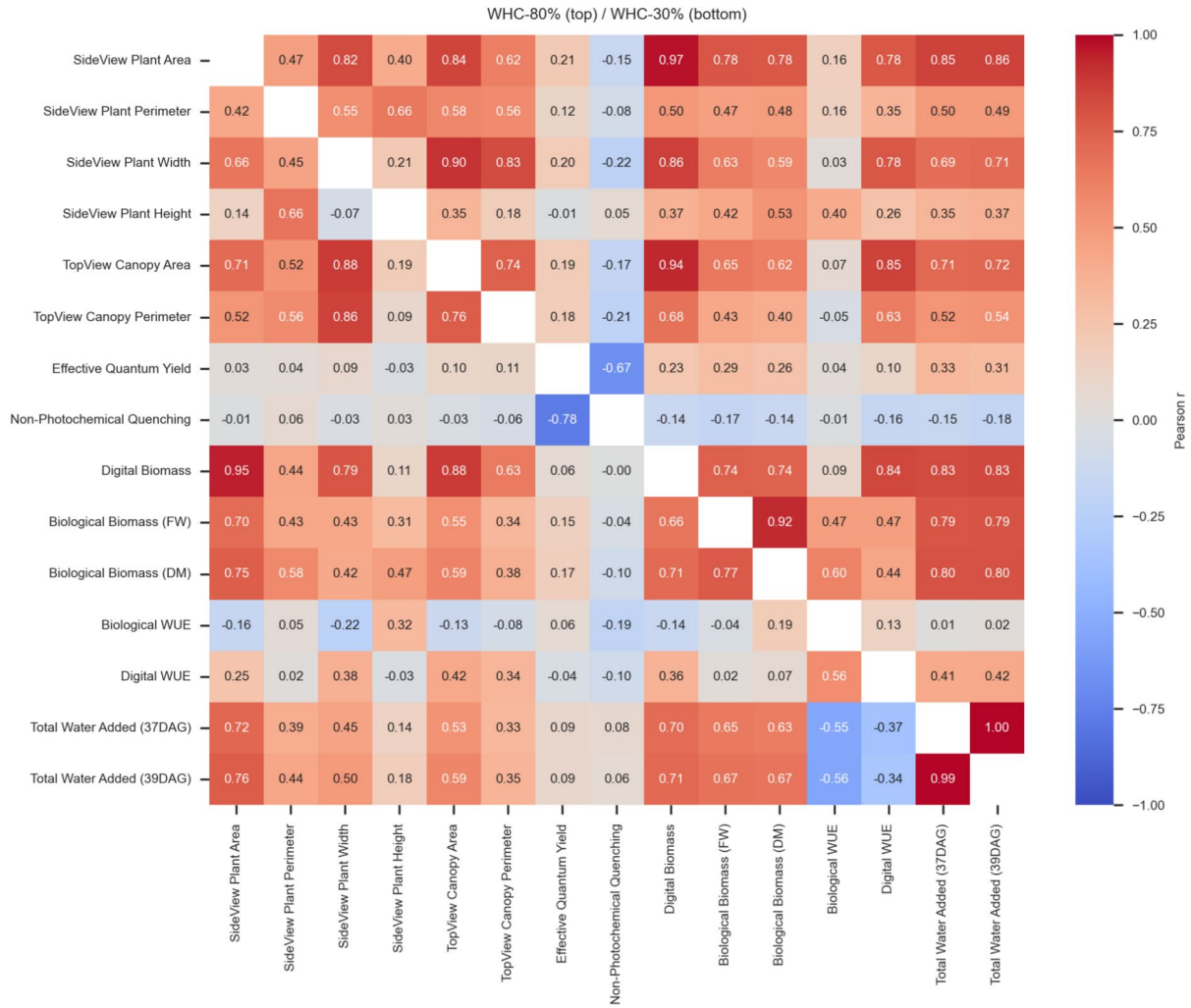

Fig. 8 Correlation matrix of the studied parameters. The values are Pearson's correlation coefficients (*r*) for traits under well watered (WHC-80%, top) and water-stress (WHC-30%, bottom) conditions. The average values of the measurements across genotypes and treatments are presented in Table S2b

captured by image-derived traits, drought-induced changes in plant architecture affecting the relationship between projected area and biomass, and temporal mismatches between time-resolved digital measurements and endpoint-based biological biomass assessments. These results suggest that while digital WUE is useful for HTPP screening, it should be interpreted with caution and not considered a direct substitute for biological WUE.

ChlF parameters showed weak correlations with growth-related traits, which may reflect a decoupling between photosynthetic performance and biomass accumulation under water deficit stress (Lawson and Vialet-Chabrand 2019). This may also be influenced by the use of discrete measurement time points, which do not fully capture the dynamic nature of photosynthetic responses to stress. ChlF parameters are highly sensitive to short-term environmental fluctuations and may therefore not directly translate into cumulative growth outcomes when assessed at limited time points (Murchie and Lawson 2013). Time-resolved analysis of ChlF parameters could provide more detailed insights into stress progression and genotype-specific responses, particularly when integrated with growth dynamics derived from imaging data.

A large proportion of the genotypes used in this study are landraces recently collected from home gardens and small-scale farms in Finland and Sweden (Leino 2023) making them highly variable in the context of outcrossing rates. The HTPP facility enabled time-resolved classification of genotypes based on plant height trajectories under water deficit using GAMs and pointwise significance analysis. This temporal classification, applied to plant height trajectories, revealed variation in water stress sensitivity, with early responders showing rapid reduction in height growth shortly after water withdrawal, and late responders maintaining height increase until soil moisture dropped below critical levels. These patterns highlight differences in drought adaptation strategies among genotypes. Late water deficit responding landraces such as Lövånger and Romfartuna could potentially be used in breeding efforts toward more drought adapted faba beans. Both accessions originated from Sweden and are characterized by early maturity. The water deficit imposed in this study represents a gradual and moderate stress scenario. Therefore, the responses observed here reflect early-stage drought adaptation under controlled growing conditions. While this approach enables precise and reproducible phenotyping, it may not fully capture plant responses to more intense or prolonged drought stress typically experienced under field conditions. Our results allowed characterising faba bean genotypes that may be used as pre-breeding materials for breeding drought-adapted germplasm.

Conclusions

This study investigated the water deficit response of a faba bean collection using an automated indoor HTPP phenotyping facility under controlled environmental conditions. Our results, derived from optimized data analysis methodologies, demonstrate that high-throughput indoor phenotyping platforms can potentially screen germplasm collections for drought adaptation-related traits while also enabling the identification of additional traits such as WUE, digital biomass, and growth dynamics. These findings support the integration of HTPP into routine crop improvement pipelines, thereby accelerating the development of climate-resilient faba bean cultivars.

Acknowledgements We would like to thank Fereshteh Dehghani and Markku Tykkyläinen, technical assistants of the glasshouse of the University of Helsinki, for their kind assistance during the experiments. The project was initiated and carried out within the framework of NordGen's grain legumes working group. We are also grateful to the staff of the seed laboratory at NordGen for preparing the main part of the seed material.

Author contributions SP: Investigation, Formal analysis, Writing—review & editing. UC-N: Funding acquisition, Resources. MO: Investigation. KH: Writing—original draft, Writing—review & editing, Supervision, Investigation, Conceptualization, Resources. HK: Writing—original draft, Writing—review & editing, Supervision, Investigation, Conceptualization, Funding acquisition. AP: Funding acquisition, Resources. IMV: Funding acquisition, Resources. GP: Funding acquisition, Resources. MWL: Funding acquisition, Resources. All authors have commented and reviewed the final manuscript.

Funding Open Access funding provided by University of Helsinki (including Helsinki University Central Hospital). This project was funded by the Nordic Genetic Resource Center (NordGen), project ID 309203, and the Research Council of Finland, Academy projects, funding decision 363375 (Fabagen).

Data availability The data will be made available upon request. All imaging and numerical data generated in this study will be deposited in PHIS (Phenotyping Hybrid Information System, http://www.phis.inra.fr/), a platform designed for the organization, management, and sharing of plant phenotyping data. This approach aims to ensure highly structured data organization in alignment with the FAIR principles (Findable, Accessible, Interoperable, Reusable), thereby fully supporting open science practices. The faba bean genetic resources used in this study are available for order from the NordGen (https://nordic-baltic-genebanks.org).

Declarations

Conflict of interest The authors declare no conflict of interest.

Consent for publication Not applicable.

Ethical approval Not applicable.

References

Alexandersson E, Keinänen M, Chawade A, Himanen K (2018) Nordic research infrastructures for plant phenotyping. Agric Food Sci 27:7–16. https://doi.org/10.23986/afsci.68870

Ali MBM, Welna GC, Sallam A, Martsch R, Balko C, Gebser B, Sass O, Link W (2016) Association analyses to genetically improve drought and freezing tolerance of faba bean (*Vicia faba* L.). Crop Sci 56:1036–1048. https://doi.org/10.2135/cropsci2015.08.0503

Al-Tamimi N, Langan P, Bernád V, Walsh J, Mangina E, Negrão S (2022) Capturing crop adaptation to abiotic stress using image-based technologies. Open Biol 12:210353. https://doi.org/10.1098/rsob.210353

Amede T, Kittlitz EV, Schubert S (1999) Differential drought responses of faba bean (*Vicia faba* L.) inbred lines. J Agron Crop Sci 183:35–45. https://doi.org/10.1046/j.1439-037x.1999.00310.x

Anshori MF, Dirpan A, Sitaresmi T, Rossi R, Farid M, Hairmansis A, Purwoko B, Suwarno WB, Nugraha Y (2023) An overview of image-based phenotyping as an adaptive 4.0 technology for studying plant abiotic stress: a bibliometric and literature review. Heliyon 9:e21650. https://doi.org/10.1016/j.heliyon.2023.e21650

Balko C, Torres AM, Gutierrez N (2023) Variability in drought stress response in a panel of 100 faba bean genotypes. Front Plant Sci 14:1236147. https://doi.org/10.3389/fpls.2023.1236147

Bevacqua E, Zappa G, Lehner F, Zscheischler J (2022) Precipitation trends determine future occurrences of compound hot–dry events. Nat Clim Change 12:350–355. https://doi.org/10.1038/s41558-022-01309-5

Blum A (2009) Effective use of water (EUW) and not water-use efficiency (WUE) is the target of crop yield improvement under drought stress. Field Crops Res 112:119–123. https://doi.org/10.1016/j.fcr.2009.03.009

Chen D, Neumann K, Friedel K, Kilian B, Chen M, Altmann T, Klukas C (2014) Dissecting the phenotypic components of crop plant growth and drought responses based on high-throughput image analysis. Plant Cell 26:4636–6455. https://doi.org/10.1105/tpc.114.129601

Chovancek E, Poque S, Bayram E, Borhan E, Jokel M, Rantanen I-M, Haznedarogly B, Himanen K, Sirin S, Allahverdiyeva Y (2025) Stepwise processing of *Chlorella sorokiniana* confers plant biostimulant that reduces mineral fertilizer requirements. Bioresour Technol 418:131923. https://doi.org/10.1016/j.biortech.2024.131923

Dodig D, Božinović S, Nikolić A, Zorić M, Vančetović J, Ignjatović-Micić D, Delić N, Weigelt-Fischer K, Altmann T, Junker A (2021) Dynamics of maize vegetative growth and drought adaptability using image-based phenotyping under controlled conditions. Front Plant Sci 12:652116. https://doi.org/10.3389/fpls.2021.652116

Gill T, Gill SK, Saini DK, Chopra Y, de Koff JP, Sandhu KS (2022) A comprehensive review of high throughput phenotyping and machine learning for plant stress phenotyping. Phenomics 2:156–183. https://doi.org/10.1007/s43657-022-00048-z

Guadarrama-Escobar LM, Hunt J, Gurung A, Zarco-Tejada PJ, Shabala S, Camino C, Hernandez P, Pourkheirandish M (2024) Back to the future for drought tolerance. New Phytol 242:372–383. https://doi.org/10.1111/nph.19619

Hatfield JL, Dold C (2019) Water-use efficiency: advances and challenges in a changing climate. Front Plant Sci 10:103. https://doi.org/10.3389/fpls.2019.00103

Horton P, Ruban AV (1992) Regulation of photosystem II. Photosynth Res 34:375–385. https://doi.org/10.1007/BF00029812

Jensen ES, Peoples MB, Hauggaard-Nielsen H (2010) Faba bean in cropping systems. Field Crops Res 115:203–216. https://doi.org/10.1016/j.fcr.2009.10.008

Ji Y, Liu Z, Cui Y, Liu R, Chen Z, Zong X, Yang T (2024) Faba bean and pea harvest index estimations using aerial-based multimodal data and machine learning algorithms. Plant Physiol 194:1512–1526. https://doi.org/10.1093/plphys/kiad577

Khan HR, Link W, Hocking TJH, Stoddard FL (2007) Evaluation of physiological traits for improving drought tolerance in faba bean (*Vicia faba* L.). Plant Soil 292:205–217. https://doi.org/10.1007/s11104-007-9217-5

Khan HR, Paull JG, Siddique KHM, Stoddard FL (2010) Faba bean breeding for drought-affected environments: a physiological and agronomic perspective. Field Crops Res 115:279–286. https://doi.org/10.1016/j.fcr.2009.09.003

Khazaei H, Vandenberg A (2020) Seed mineral composition and protein content of faba beans (*Vicia faba* L.) with contrasting tannin contents. Agronomy 10:511. https://doi.org/10.3390/agronomy10040511

Khazaei H, Street K, Bari A, Santanen A, Stoddard FL (2013) Do faba bean (*Vicia faba* L.) accessions from environments with contrasting seasonal moisture availabilities differ in stomatal characteristics and related traits? Genet Resour Crop Evol 60:2343–2357. https://doi.org/10.1007/s10722-013-0002-4

Khazaei H, O'Sullivan DM, Sillanpää MJ, Stoddard FL (2014) Use of synteny to identify candidate genes underlying QTL controlling stomatal traits in faba bean (*Vicia faba* L.). Theor Appl Genet 127:2371–2385. https://doi.org/10.1007/s00122-014-2383-y

Khazaei H, Link W, Street K, Stoddard FL (2018) ILB 938, a valuable faba bean (*Vicia faba* L.) accession. Plant Genet Resour 16:478–482. https://doi.org/10.1017/S1479262118000205

Kim M, Lee C, Hong S, Kim SL, Baek J-H, Kim K-H (2021) High-throughput phenotyping methods for breeding drought-tolerant crops. Int J Mol Sci 22:8266. https://doi.org/10.3390/ijms22158266

Klukas C, Chen D, Pape J-M (2014) Integrated analysis platform: an open-source information system for high-throughput plant phenotyping. Plant Physiol 165:506–518. https://doi.org/10.1104/pp.113.233932

Lawson T, Vialet-Chabrand S (2019) Speedy stomata, photosynthesis and plant water use efficiency. New Phytol 221:93–98. https://doi.org/10.1111/nph.15330

Leino MW (2023) *Vicia faba* plant genetic resources preserved in home gardens in Sweden. Legume Perspect 24:13–14

Mandour H, Khazaei H, Stoddard FL, Dodd IC (2023) Identifying physiological and genetic determinants of faba bean transpiration response to evaporative demand. Ann Bot 131:533–544. https://doi.org/10.1093/aob/mcad006

Mansoor S, Chung YS (2024) Functional phenotyping: understanding the dynamic response of plants to drought stress. Curr Plant Biol 38:100331. https://doi.org/10.1016/j.cpb.2024.100331

Mohammadi S, Uhlen AK, Lillemo M, Ergon Å, Shafiee S (2024) Enhancing phenotyping efficiency in faba bean breeding: integrating UAV imaging and machine learning. Precis Agric 25:1502–1528. https://doi.org/10.1007/s11119-024-10121-4

Murchie EH, Lawson T (2013) Chlorophyll fluorescence analysis: a guide to good practice and understanding some new applications. J Exp Bot 64:3983–3998. https://doi.org/10.1093/jxb/ert208

Nagel KA, Putz A, Gilmer F, Heinz K, Fischbach A et al (2012) GROWSCREEN-Rhizo is a novel phenotyping robot enabling simultaneous measurements of root and shoot growth for plants grown in soil-filled rhizotrons. Funct Plant Biol 39:891–904. https://doi.org/10.1071/FP12023

Neumann K, Klukas C, Friedel S, Rischbeck P, Chen D, Entzia A, Stein N, Graner A, Kilian B (2015) Dissecting spatiotemporal biomass accumulation in barley under different water regimes using high-throughput image analysis. Plant Cell Environ 38:1980–1996. https://doi.org/10.1111/pce.12516

Peltonen-Sainio P, Juvonen J, Korhonen N, Parkkila P, Sorvali J, Gregow H (2021) Climate change, precipitation shifts and early summer drought: an irrigation tipping point for Finnish farmers? Climate Risk Manag 33:100334. https://doi.org/10.1016/j.crm.2021.100334

Piepho H-P (2004) An algorithm for a letter-based representation of all-pairwise comparisons. J Comput Graph Stat 13:456–466. https://doi.org/10.1198/1061860043515

Pieruschka R, Schurr U (2019) Plant phenotyping: past, present, and future. Plant Phenomics 2019:7507131. https://doi.org/10.34133/2019/7507131

Pollari M, Sipari N, Poque S, Himanen K, Mäkinen K (2022) Effects of Poty-potexvirus synergism on growth, photosynthesis and metabolite status of *Nicotiana benthamiana*. Viruses 15:121. https://doi.org/10.3390/v15010121

R Core Team 2025 R: a language and environment for statistical computing R foundation for statistical computing Vienna, Austria 10.32614/R

Rahaman MM, Ahsan MA, Gillani Z, Chen M (2017) Digital biomass accumulation using high-throughput plant phenotype data analysis. J Integr Bioinform 14:20170028. https://doi.org/10.1515/jib-2017-0028

Roitch T, Himanen K, Chawade A, Jaakola L, Nehe A, Alexandersson E (2022) Functional phenomics for improved climate resilience in Nordic agriculture. J Exp Bot 73:5111–5127. https://doi.org/10.1093/jxb/erac246

Shapiguzov A, Punkkinen M, Laine T, Engström S, Aphalo PJ, Khazaei H (2026) Linking stomatal function with photosynthetic light reactions and stress response in faba bean. Environ Exp Bot 241:106290. https://doi.org/10.1016/j.envexpbot.2025.106290

Sozzani R, Busch W, Spalding EP, Benfey PN (2014) Advanced imaging techniques for the study of plant growth and development. Trends Plant Sci 19:304–310. https://doi.org/10.1016/j.tplants.2013.12.003

Spinoni J, Vogt JV, Naumann G, Barbosa P, Dosio A (2018) Will drought events become more frequent and severe in Europe? Int J Climat 38:1718–1736. https://doi.org/10.1002/joc.5291

Swarup S, Cargill EJ, Crosby K, Flagel L, Kniskern J, Glenn KC (2021) Genetic diversity is indispensable for plant breeding to improve crops. Crop Sci 61:839–852. https://doi.org/10.1002/csc2.20377

Thoday-Kennedy E, Joshi S, Daetwyler HD, Hayden M, Hudson D, Spangenberg G, Kant S (2021) Digital phenotyping to delineate salinity response in safflower genotypes. Front Plant Sci 12:662498. https://doi.org/10.3389/fpls.2021.662498

Tschiersch H, Junker A, Meyer RC, Altmann T (2017) Establishment of integrated protocols for automated high throughput kinetic chlorophyll fluorescence analyses. Plant Methods 13:54. https://doi.org/10.1186/s13007-017-0204-4

van Rij J, Wieling M, Baayen R, van Rijn H (2022) itsadug: Interpreting time series and autocorrelated data using GAMMs. R package version 2.4.1. https://doi.org/10.32614/CRAN.package.itsadug

Visakh R, Anand S, Reddy S, Jha U, Sah R, Beena R (2024) Precision phenotyping in crop science: from plant traits to gene discovery for climate-smart agriculture. Plant Breed. https://doi.org/10.1111/pbr.13228

Waskom ML (2021) Seaborn: statistical data visualization. J Open Source Softw 6:3021. https://doi.org/10.21105/joss.03021

Wickham H (2016) ggplot2: Elegant graphics for data analysis. Springer-Verlag New York, USA. R 550 package version 3.5.2. https://doi.org/10.32614/CRAN.package.ggplot2

Wood SN (2011) Fast stable restricted maximum likelihood and marginal likelihood estimation of semiparametric generalized linear models. J Royal Statist Soc (b) 73:3–36. https://doi.org/10.1111/j.1467-9868.2010.00749.x